Directionality Indices: Testing Information Transfer with Surrogate Correction

Beth Jelfs* and Rosa H. M. Chan
Department of Electronic Engineering and
Centre for Biosystems, Neuroscience, & Nanotechnology,
City University of Hong Kong
(Dated: November 5, 2017)

Directionality indices can be used as an indicator of the asymmetry in coupling between systems and have found particular application in relation to neurological systems. The directionality index between two systems is a function of measures of information transfer in both directions. Here we illustrate that before inferring the directionality of coupling it is first necessary to consider the use of appropriate tests of significance. We propose a surrogate corrected directionality index which incorporates such testing. We also highlight the differences between testing the significance of the directionality index itself versus testing the individual measures of information transfer in each direction. To validate the approach we compared two different methods of estimating coupling, both of which have previously been used to estimate directionality indices. These were the modeling based evolution map approach and a conditional mutual information (CMI) method for calculating dynamic information rates. For the CMI based approach we also compared two different methods for estimating the CMI, an equi-quantization based estimator and a k-nearest neighbors estimator.

I. INTRODUCTION

Measures of the connectivity between coupled systems have garnered interest in disciplines from finance [1] to ecology [2] and have become a key topic of research in neuroscience, with connectivity measures being used to assess neural data from various different modalities including electroencephalography (EEG) [3–6], functional magnetic resonance imaging (fMRI) [7], electrocorticography (ECoG) [8, 9] and local field potentials (LFP) [10–12]. The research not only spans different modalities but also focuses on different premises regarding connectivity: causal relationships [10, 12], synchronization between systems [3–5], or the information flow [5, 6, 11, 12] or information transfer [12] across systems. At their heart, however, all attempt to quantify the relationship and interdependencies between multiple (sub)systems within the brain.

Methods for studying the relationships between coupled systems range from simple measures of correlation and coherence to more complex measures [4, 13]. Many commonly used methods are based upon Granger causality [14] such as partial coherence [15], directed transfer functions [16] and extensions thereof. Alternative approaches include measures of synchrony using both phase [17] and state space [3], or measures of directionality including information theoretic measures such as mutual information [18], Kullback-Leibler divergence [19] and transfer entropy [20]. Each have their strengths and limitations depending on the scenario. For instance some methods may give information regarding the existence of a relationship without knowledge about the directionality (e.g. correlation and coherence based measures) or may only be appropriate for linear models (e.g. standard Granger causality based measures). In fact, different families of measures may present us with slightly different information regarding the data in question, thereby giving a more complete understanding of the relationship [4]. Rather than focus on the individual connectivity measures the aim of this paper is to investigate the use and applicability of such methods in the creation of directionality indices, with particular focus on their use with field potential recordings of neural systems.

A directionality index provides an indication of the asymmetry in the coupling between two systems. It is the normalized difference between the measures of the strength of interaction in each direction. That is,

$$D_{1\to 2} = \frac{I_{1\to 2} - I_{2\to 1}}{I_{1\to 2} + I_{2\to 1}}, \tag{1}$$

where $I_{1\to 2}$ is the measure of how the first system drives the second and $I_{2\to 1}$ is the same measure in the opposite direction. The directionality index, $D_{1\to 2}$, ranges from -1 to 1, with a value of 1 indicating unidirectional coupling between the two systems in the direction $1 \to 2$ and a value of -1 indicating the reverse is true, unidirectional coupling in the direction $2 \to 1$. Hence, the accuracy of the method used to calculate the strength of interaction in each direction will have a significant impact on the efficacy of the directionality index to quantify the relationship.

Numerous methods have been used to quantifying the interactions of synchronized systems and their outcomes compared and contrasted [3, 4, 21] but when considering continuous neural systems it can be more appropriate to model them as weakly coupled oscillators [22, 23]. Changes in the dynamics of weakly coupled systems can be observed in their phase before either the amplitude or frequency. Analyzing the data in terms of the phase interactions allows for small initial changes in the dynamics between the systems to be detected, and accura-

* Current Affiliation: School of Engineering, RMIT University, Melbourne, Australia; beth.jelfs@rmit.edu.au

tely modeled, significantly earlier than alternative approaches. This study uses two different methods of estimating phase interactions: a model fitting approach that represents the coupling as a two dimensional noisy map, called the evolution map approach (EMA) [24]; and an information theoretic approach using conditional mutual information (CMI) [25].

In relation to determining the directionality of coupling it is important to have a clear perspective of what exactly is to be measured. In many instances the terms causality, information flow and information transfer are used almost interchangeably. From an information theoretic point of view information transfer is one of the three components of information flow (the other two being storage and modification) and although many methods have been used to measure the so called "information flow", including those used in this study, it is not clear that they truly measure the complete information flow [26, 27]. At the same time causal interactions can occur without information transfer, however, information transfer cannot occur without a causal interaction [28], hence absence of information transfer does not prove the absence of a causal relationship. However, in terms of neural connectivity, it may be that information transfer is the component of information flow we are most interested in when considering brain dynamics and the computational processes involved [29]. Therefore, although previous work has used the term information flow when describing the directionality indices we have instead more precisely termed them as measures of predictive information transfer.

In this study we compare and contrast the use of phase based information transfer measures EMA and CMI to assess the directionality of coupling. Despite both methods having previously been used to create directionality indices for use with neurological data [8, 30, 31] and the results from both methods having been shown for cardiorespiratory data [32] no thorough comparison of the methods has been undertaken. To demonstrate the efficacy of the approaches a simple model of two weakly coupled oscillators is used with a number of scenarios: unidirectional coupling; bidirectional coupling; and discrepancies between the fundamental frequencies of the oscillators. The different parameters of the EMA and CMI methods are studied to assess their impact on the sensitivity of the algorithms to detect asymmetry in the coupling. For completeness we also consider the effect of the choice of estimator used in the CMI calculation by comparing a marginal equi-quantization with an extension of the k-nearest neighbor (kNN) method for mutual information from [18].

Our findings show the necessity for the use of appropriate surrogate data when creating a directionality index, a crucial step in the assessment of any neural data where underlying system dynamics may be unknown. We propose a method for effectively adjusting the directionality index after surrogate data testing of the results in each of the individual directions. This ensures a more reliable indicator of the relationship between the two systems.

The paper is organised as follows: Sections II and III introduce the EMA and CMI estimators and their directionality indices, respectively. Section IV describes the systems used to test the directionality indices, the surrogate data and the proposed correction to the directionality indices using the surrogate data. Results illustrating the impact of the surrogate correction are given in Section V and finally, Section VI concludes the paper.

II. EVOLUTION MAP APPROACH

One simple yet effective method for measuring the direction of the interaction between the phases of weakly coupled oscillators is the evolution map approach (EMA) based on the work by Rosenblum and Pikovsky [24] whereby the relationship between the two systems is represented by a two dimensional noisy map. If we consider the phase model of the continuous phase variables, $\phi_1(t)$ and $\phi_2(t)$ with natural frequencies ω_1 and ω_2 respectively as

$$\begin{aligned}\dot{\phi}_1 =&\omega_1 + \varepsilon_1 f_1\left(\phi_1, \phi_2\right) + \xi_1(t),\\ \dot{\phi}_2 =&\omega_2 + \varepsilon_2 f_2\left(\phi_2, \phi_1\right) + \xi_2(t),\end{aligned} \tag{2}$$

then the coupling is described by the periodic functions f_1 and f_2 and the strength of coupling by the parameters ε_1 and ε_2, with ξ_1 and ξ_2 defining the random (aperiodic) amplitude fluctuations.

The phase increments of the time series over a constant time interval τ can then be defined as

$$\begin{aligned}\Delta_\tau\phi_1(k) =&\phi_1(t_k+\tau) - \phi_1(t_k)\\ =&\mathcal{F}_1[\phi_1(t_k), \phi_2(t_k)] + \eta_1(t_k),\\ \Delta_\tau\phi_2(k) =&\phi_2(t_k+\tau) - \phi_2(t_k)\\ =&\mathcal{F}_2[\phi_2(t_k), \phi_1(t_k)] + \eta_2(t_k),\end{aligned} \tag{3}$$

where $\mathcal{F}_1$ and $\mathcal{F}_2$ represent the phase dependencies between the two oscillators. Due to the cyclic nature of the phases ϕ_1 and ϕ_2 a finite Fourier series

$$F_{1,2} = \sum_{m,l} A_{m,l} e^{im\phi_1 + il\phi_2}, \tag{4}$$

can be used to fit, in a least mean squares sense, the dependencies of the increments $\Delta_\tau\phi_1$ and $\Delta_\tau\phi_2$ on the phases ϕ_1, ϕ_2. Using the fitting to approximate F_1 and F_2 the cross dependences of the phase dynamics are then estimated as

$$\begin{aligned}c_1^2 &= \int_0^{2\pi}\int_0^{2\pi}\left(\frac{\partial F_1}{\partial\phi_2}\right)d\phi_1 d\phi_2,\\ c_2^2 &= \int_0^{2\pi}\int_0^{2\pi}\left(\frac{\partial F_2}{\partial\phi_1}\right)d\phi_1 d\phi_2.\end{aligned} \tag{5}$$

The directionality index is then calculated in terms of the coefficients c_1 and c_2 as

$$D_{1\to 2} = \frac{c_2 - c_1}{c_2 + c_1}. \tag{6}$$

The EMA has previously been used to assess the neuronal oscillations of rhythmical activity [33], cardio-respiratory interactions [34], ECoG of hand movements [8] and different frequency bands of LFP data from rats [31]. In [34] the EMA was compared with an instantaneous period approach and a mutual prediction approach and was found to be generally more stable in terms of variation for a range of noise intensities and coupling strengths, and when assessing the difference between coupled and uncoupled systems with common driving. An extended EMA which allows improved performance for short noisy time series has been proposed in [35] and semi-empirically determined confidence intervals provided. A comparison between this approach and an alternative state space approach suggested that for weak phase diffusion with low noise levels and short time series the phase based approach is superior, however, in general both have strengths and weaknesses dependent on the time series in question [36].

In terms of the parameters of the algorithm, the estimator has generally been considered to have only one parameter, the time lag, τ which defines the size of the phase increments. The order of the Fourier series used to fit the dependencies, has not previously been considered as part of the estimator - typically a model order of 3 has been used. In [24] it was stated that the size of the increments τ was not important provided it was within a range of approximately 0.5-50 periods of oscillation, however, [34] recommend a value of $\tau = 1$ period. In this study we consider the impact of the order of the Fourier series on the accuracy of the least mean square fit as well as a range of different τ.

III. CONDITIONAL MUTUAL INFORMATION

An alternative approach to the EMA is to consider the interactions of the phases from an information theoretic point of view rather than a model fitting one. For two coupled systems X and Y where the time series $\{x(t)\}$ and $\{y(t)\}$ are individual realizations of the systems, the mutual information $I\left(x(t); y(t+\tau)\right)$ represents the amount of information contained in X about Y in its future τ time units ahead. However, if X and Y are not independent this measure could also contain information about the future of Y contained in the process itself. By conditioning the mutual on the time series $y(t)$ to give the conditional mutual information (CMI)

$$I\big(x(t); y(t+\tau)\big|y(t)\big), \tag{7}$$

we have the information contained in X about the future of Y, not including the history of Y contained within Y itself or their shared history. In this way the CMI can be considered an information theoretic formulation of Granger causality and also has an equivalence with transfer entropy [37]. For a general review of information theoretic approaches to causality see [38].

To investigate the directionality of coupling requires information about how the dynamics of one system influences the other, for this purpose coarse-grained information rates can be used. Coarse-grained information rates provide measures of the regularity and predictability of systems. They are inversely proportional to coarse-grained entropy rates (measures of chaoticity or complexity) which can be used to classify states of chaotic systems in the same way as the Kolmogorov-Sinai entropy can [5]. Coarse-grained information rates are defined in terms of the mutual information norm and have been shown to be more robust to noise and less computationally complex than alternatives such as Lyapunov exponents. To calculate the coarse grained information rate the average of the CMI over a range of values of τ is taken to give

$$i\left(X, Y|Y\right) = \frac{1}{\tau_{\max}} \sum_{\tau=1}^{\tau_{\max}} I(x; y_\tau|y), \tag{8}$$

where $x = x(t)$, $y = y(t)$ and $y_\tau = y(t+\tau)$ and $\tau_{\max}$ is usually defined in terms of the maximum value of τ for which the information between y and y_τ is non zero.

To calculate the directionality index from the instantaneous phases as in (3) and in line with the approach from [25] we consider the phases in terms of their phase increments

$$\begin{aligned} \Delta_\tau\phi_1 =& \phi_1(t+\tau) - \phi_1(t) \\ \Delta_\tau\phi_2 =& \phi_2(t+\tau) - \phi_2(t). \end{aligned} \tag{9}$$

Replacing the time series with the phases in (8) gives the information rates in each direction as

$$\begin{aligned} i\left(1 \to 2\right) =& \frac{1}{\tau_{\max}} \sum_{\tau=1}^{\tau_{\max}} I(\phi_1; \Delta_\tau\phi_2|\phi_2) \\ i\left(2 \to 1\right) =& \frac{1}{\tau_{\max}} \sum_{\tau=1}^{\tau_{\max}} I(\phi_2; \Delta_\tau\phi_1|\phi_1), \end{aligned} \tag{10}$$

finally a directionality index is constructed in the same manner as for the EMA

$$D_{1\to2} = \frac{i(1\to2) - i(2\to1)}{i(1\to2) + i(2\to1)}. \tag{11}$$

The problem of estimating CMI can be defined in terms of estimating a series of entropies and then computing the CMI. The CMI can be defined in terms of entropies as

$$I(X;Y|Z) = H(X,Z) + H(Y,Z) - H(Z) - H(X,Y,Z). \tag{12}$$

Estimation of the entropies requires accurate calculation of the probability density functions of the data. For this purpose we compare two different methods, one non-parametric and one parametric. The non-parametric method is based upon equi-quantization and the parametric on k-nearest neighbors (kNN). Although a number of alternative estimation methods exist (see [38]) these methods have been selected as they have previously been shown to provide reliable estimates of CMI [39].

The non-parametric equi-quantization method is a binning method based upon dividing the sample space into a set number of equi-probable bins. The data is first sorted by magnitude and then partitioned such that all the bins contain approximately the same number of data points. The equi-quantization method was previously shown to provide robust estimates of CMI with relatively small variance albeit at the expense of having a higher bias [39].

The parametric kNN method is an extension of the approach from [18] for estimating mutual information. The kNN method has previously been applied to the estimation of CMI for state space reconstructions [40] and also to phase data where it was shown to provide accurate results with a relatively low bias albeit with some sensitivity to the choice of the number of neighbors [39]. However, the kNN algorithm for estimating mutual information provides two different approaches, one based upon estimating the k neighbors from a square neighborhood the other using a rectangular neighborhood. As the rectangular version has been shown to be better suited to higher dimensional data [18] - which in terms of neurological data with recordings from multiple electrodes may well be an issue - we have opted to extend the rectangular version to the estimation of CMI details. Following a similar approach to the extension of the mutual information estimator to the estimation of transfer entropy in [41] we get an estimator of the CMI given by

$$\begin{aligned} I(X;Y|Z) =& H(X,Z) + H(Y,Z) - H(Z) - H(X,Y,Z) \\ =& \psi(k) - \frac{d_x + d_y + d_z - 1}{k} + \\ & \Big\langle -\psi(n_{xz}) - \psi(n_{yz}) + \psi(n_z) \\ & + \frac{d_x + d_z - 1}{n_{xz}} + \frac{d_y + d_z - 1}{n_{yz}} - \frac{d_z - 1}{n_z} \Big\rangle, \end{aligned} \tag{13}$$

where $< \ldots >$ denotes the average over $i \in [1, \ldots, N]$ and over all realizations. Details of the derivation of this estimator are given in the appendix.

IV. NUMERICAL EXPERIMENTS

Numerical experiments were performed for a number of different scenarios with data generated from a coupled pair of Rössler systems [42]. The Rössler model has previously been used in the study of the interactions of coupled oscillators and to test the effectiveness of both the EMA and CMI directionality indices [24, 25].

In each of the scenarios described below we investigated the impact of the parameters on the accuracy of the methods. For all three methods the time lag defining the size of the phase increments was addressed by adjusting the value of τ in the EMA and the value of $\tau_{\max}$ for which the estimates are averaged across for the CMI methods. For the EMA we also varied the model order of the Fourier series used to fit the data dependencies and for the CMI/CMI-kNN the number of quantizations/nearest neighbors used in the probability density function estimates, respectively. The effect of the coupling strength was not considered as both the EMA and CMI methods of detecting phase based directionality are known to fail in the presence of synchronization, see [24, 25].

TABLE I. Parameters of the Rössler systems.

System	Coupling	Direction	ω_1	ω_2	ϵ_1	ϵ_2
1	unidirectional	$1 \to 2$	0.85	1.15	0	0.05
2	unidirectional	$1 \to 2$	0.5	2.515	0	0.1
3	unidirectional	$2 \to 1$	0.5	2.515	0.1	0
4	bidirectional	$1 \to 2$	0.85	1.15	0.01	0.02
5	bidirectional	$2 \to 1$	0.85	1.15	0.01	0.005
6	bidirectional	equivalent	0.85	1.15	0.01	0.01

A. Systems

The coupled Rössler model is described by [43, 44]

$$\begin{aligned} \dot{x}_{1,2} =& -\omega_{1,2} y_{1,2} - z_{1,2} + \epsilon_{1,2}\left(x_{2,1} - x_{1,2}\right), \\ \dot{y}_{1,2} =& \omega_{1,2} x_{1,2} + 0.15 y_{1,2}, \\ \dot{z}_{1,2} =& 0.2 + z_{1,2}(x_{1,2} - 10), \end{aligned} \tag{14}$$

where $\omega_{1,2}$ are the fundamental frequencies of the oscillators and ϵ describes the strength of the coupling. To cover a number of scenarios we generate systems based on six different sets of parameters, listed in Table I. For every system 100 random initializations were generated each with 10,000 data points and approximately 20 samples per period. The resulting 500 periods of oscillation have previously been shown to be sufficient for accurate estimation using the EMA [24] with the CMI requiring less data [39]. Instantaneous phases of the systems were generated from the analytic signals of $\dot{x}_{1,2}$ obtained via the Hilbert transform. Of the systems outlined in Table I, the first three all had unidirectional coupling between the oscillators.

1. The first system is a straightforward unidirectional coupling of two roughly equivalent oscillators with the coupling from oscillator 1 to oscillator 2.

2. The second system has an imbalance in the ratio of the frequencies of the two oscillators of approximately 1:5, the coupling in the system remains from oscillator 1 to oscillator 2, meaning the coupling is from the slower oscillator to the faster.

3. The third system is the same system as system 2 but with the direction of the coupling reversed so that the direction of coupling is now from oscillator 2, with the faster frequency of oscillation, to oscillator 1, with the slower frequency of oscillation.

The last three systems all have oscillators of roughly equivalent frequency but this time with bidirectional coupling.

4. The coupling in System 4 is in both directions but with stronger coupling in the direction of oscillator 1 to oscillator 2.

5. For the next system the coupling strengths are lower than those in System 4 and with the direction of the stronger coupling reversed so as to be in the direction of oscillator 2 to oscillator 1.

6. The coupling strengths in the final system are equivalent in both directions.

All the systems have previously been used to investigate the performance of the CMI methods. Systems 1-3 have been used to assess the effect of the number of data samples and size of the bins/number of neighbors for both the CMI and a variant of the CMI-kNN method [39], whereas systems 4-6 have been used to asses the effects of the data length, quantization and length of the lag for the CMI directionality index [25].

B. Surrogate Data

To test the significance of the results obtained from all three approaches, a surrogate data method was used. Surrogate data time series have the same statistical properties as the original data but with all dependencies destroyed [45, 46]. In this case the surrogate data was generated using an iterative amplitude adjusted FFT (iAFFT) to preserve both the amplitude and frequency distributions of the data [47]. For each pair of time series in the original data, the data of the driving system was left unaltered and surrogates of the driven system were created.

Having obtained a set of surrogate data with the same properties as the original data but with no causal relationship, the directionality results for the surrogates are obtained and a distribution of the values created. From these results a range of values which the surrogate data is expected to take can be defined. Identifying whether the directionality results of the original data fall outside the expected range of the surrogate data gives a determination of whether the results are significant or whether by using these results we may be incorrectly inferring a causal relationship. Setting an interval of ± 2 standard deviations around the mean of the surrogate data gives an assumption that 95% of the surrogate data should fall within this range and hence we can infer confidence that any results falling outside of this region correctly identify the direction of the causal relationship.

However, how best to determine the surrogate data range for the directionality indices needs to be considered. Surrogate data testing of directionality indices can be approached in two different manners, one is to test the directionality index itself against the directionality indices generated using the surrogate data. The second approach is to test each measure of the coupling against the surrogate data before calculating the directionality index. A number of surrogate data generation approaches have been considered when testing the statistical validity of CMI results; including Fourier transform based surrogate data generation methods [39, 48]. While neither [39] or [48] created directionality indices both tested the significance of the individual measures of coupling generated using the CMI method. Alternatively, [25] took the approach of testing directly on the directionality indices created from the surrogate data. To the best of our knowledge nobody has yet tested the EMA method against surrogate data to check the statistical validity of the results.

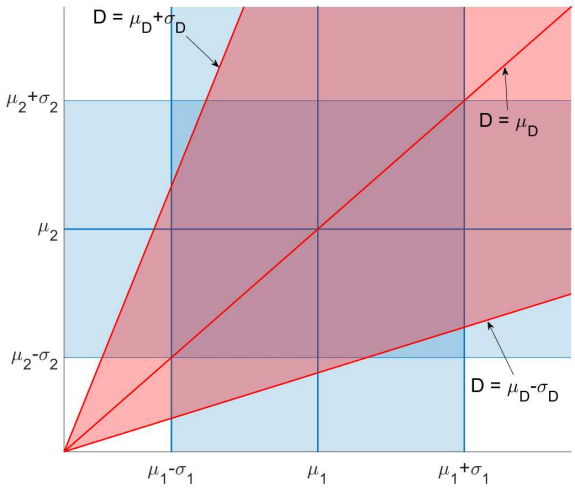

FIG. 1. Comparison of surrogate data regions for D and $I_{1\to2}$ and $I_{2\to1}$.

Figure 1 shows a range of values of $I_{1\to2}$ and $I_{2\to1}$ with specified means, μ_1 and μ_2, and standard deviations σ_1 and σ_2. The shaded regions indicate the areas covered by $\mu_{1,2} \pm \sigma_{1,2}$, which in this case relates to the area within which approximately 68% of the surrogate data can be expected to fall. Using the same example values of $I_{1\to2}$ and $I_{2\to1}$ directionality indices $D_{1\to2}$ were calculated and a mean μ_D and standard deviation σ_D of the indices estimated. Plotting the values of $\mu_D \pm \sigma_D$ as functions of $I_{1\to2}$ and $I_{2\to1}$ it can be seen that there are areas covered by the regions $I_{1\to2} = \mu_1 \pm \sigma_1$ and $I_{2\to1} = \mu_2 \pm \sigma_2$ which are not covered by the region $D = \mu_D \pm \sigma_D$. This includes regions (where either $I_{1\to2}$ is close to $\mu_1 - \sigma_1$ and $I_{2\to1}$ is close to $\mu_2 + \sigma_2$ or $I_{1\to2}$ is close to $\mu_1 + \sigma_1$ and $I_{2\to1}$ is close to $\mu_2 - \sigma_2$) where data which would fall inside the range of the surrogate data for both $I_{1\to2}$ and $I_{2\to1}$ is outside of the range of the surrogate data if testing against the values of $D_{1\to2}$. This holds true for all multiples of σ. Therefore, it is necessary rather than testing against the directionality indices created from the surrogate data to first test each individual direction before calculating the directionality indices.

Here we propose an adjustment to how the directionality index is created based upon the results of the tests for statistical significance. First $I_{1\to2}$ and $I_{2\to1}$ are tested against the surrogate data. If the result can be considered to be more significant than just the result of any bias in the estimator then it is left as it is, otherwise it is set to 0. The corrected directional results for $I_{1\to2}$ are given by

$$I_{1\to2_{\text{corr}}} = \begin{cases} I_{1\to2} & \text{if } I_{1\to2} > \mu_1 + \sigma_1, \\ I_{1\to2} & \text{if } I_{1\to2} < \mu_1 - \sigma_1, \\ 0 & \text{otherwise,} \end{cases} \tag{15}$$

where μ_1 and σ_1 are the mean and standard deviation of the estimates of $I_{1\to2}$ from the surrogate data, the same correction is performed for $I_{2\to1}$. Using these corrected values the directionality index can be estimated as in (1). In this case the corrected value would result in values of 1 and -1 indicating unidirectional couplings as before, a value of 0 for equivalent bidirectional coupling and an undefined result when there is no coupling present.

V. RESULTS

A. Unidirectional Coupling

As an initial test, directionality indices using both the original and the surrogate corrected formulation of $D_{1\to2}$, were calculated for 100 different initializations of the unidirectionally coupled equivalent Rössler oscillators described as System 1 in Section IV A. The average value of $D_{1\to2}$ for a range of different parameters of the three test algorithms are illustrated in Fig. 2. For the EMA algorithm the model order of the Fourier series ranged from 1:10. For the CMI and CMI-kNN the quantization or k-nearest neighbors took values of 2, 4, 8, 16, 32 and 64. The mutual information between the data and lagged versions of itself were calculated and a lag value of 120 was determined to be the point where the mutual information became approximately zero. Hence, the maximum lag $\tau_{\max}$ the CMI was averaged across to obtain the information rates were selected to be from 10 to 120 in steps of 10. Due to the difference in the set-up of the EMA a finer graining in the lag value, τ, was selected for small values of the lag, with initial steps of one for lags 1 to 20 after which larger steps of 10 were tested for 30 to 120.

As can be seen from Fig. 2 the majority of parameter settings gave a correct indication of the direction of coupling, albeit with smaller values for the original formulations (Fig. 2a, 2c, 2e). Figures 2a and 2b show that on the whole the EMA values were lower than the comparable results from other methods and that the smaller model orders of the original EMA gave incorrect indications of the direction of coupling. The only setting of the recalibrated directionality indices to give incorrect results was for the very small value of $k = 2$ for CMI-kNN (Fig. 2f) which became unreliable results as the value of the maximum lag increases due to the limited accuracy of the probability distribution estimated from only two neighbors.

Closer analysis of the distribution of the results reveals a noticeable difference between the EMA and CMI approaches. Table II shows the parameters of the algorithms which gave the most successful results across all lags. For each algorithm the percentage of correct directionality indices for both the original and recalibrated versions are shown, along with the percentages of the results which are outside the range obtained from 100 different surrogates for each instance. For the original indices the percentage of the indices themselves outside of the range of the surrogate generated indices are given whereas for the recalibrated indices the percentage of the measures in each direction are given. The results illustrate that there are parameters of both CMI estimators which result in 100% correct directionality indices. The differences in the formulation of the original and the recalibrated indices mean that while results in the correct direction must be by default outside of the range of the surrogates in at least one direction for the recalibrated version, this is not the case for the original formulation. This can be seen for the CMI-kNN where although the results may all be in the correct direction when considering the original formulation there is a slightly lower maximum of 99% of results outside of the range of the surrogate data. However, these results fall within the range of what may be expected due to chance, unlike the EMA. The best combination achieved with the original EMA was 93% and occurred for a model order of 9 at lag $\tau = 10$. The recalibrated version gave 33% correct also at an order of 9 but with a lag of $\tau = 90$. In both cases the number of these results which were outside of the range of the surrogates was only 33%.

Based on the results from the first system while all the methods gave correct results the EMA did not provide results which were consistently statistically valid. Comparing the CMI methods, the original directionality indices proved to have greater sensitivity to the parameters of the algorithms. Table II shows only the results from the best performing parameters of the algorithms, however, for the recalibrated directionality indices similar results were also obtained for the CMI algorithm with $q = 4$ and $q = 16$ and for the kNN version for $k = 16$ and $k = 64$. In contrast the performance of the original CMI algorithms deteriorated with any change in the values of q and k, and showed greater variability in the significance of the results dependent on the maximum lag chosen.

Table II illustrates that for the CMI methods when using the corrected directionality indices it is possible to obtain a correct indication of the direction of coupling based on the results from only one direction. In this case only the coupling in the direction $1 \to 2$ consistently gave results outside of the range of the surrogates with a maximum of 8% of results in the opposite direction outside of the range of the surrogates. In contrast, Table III

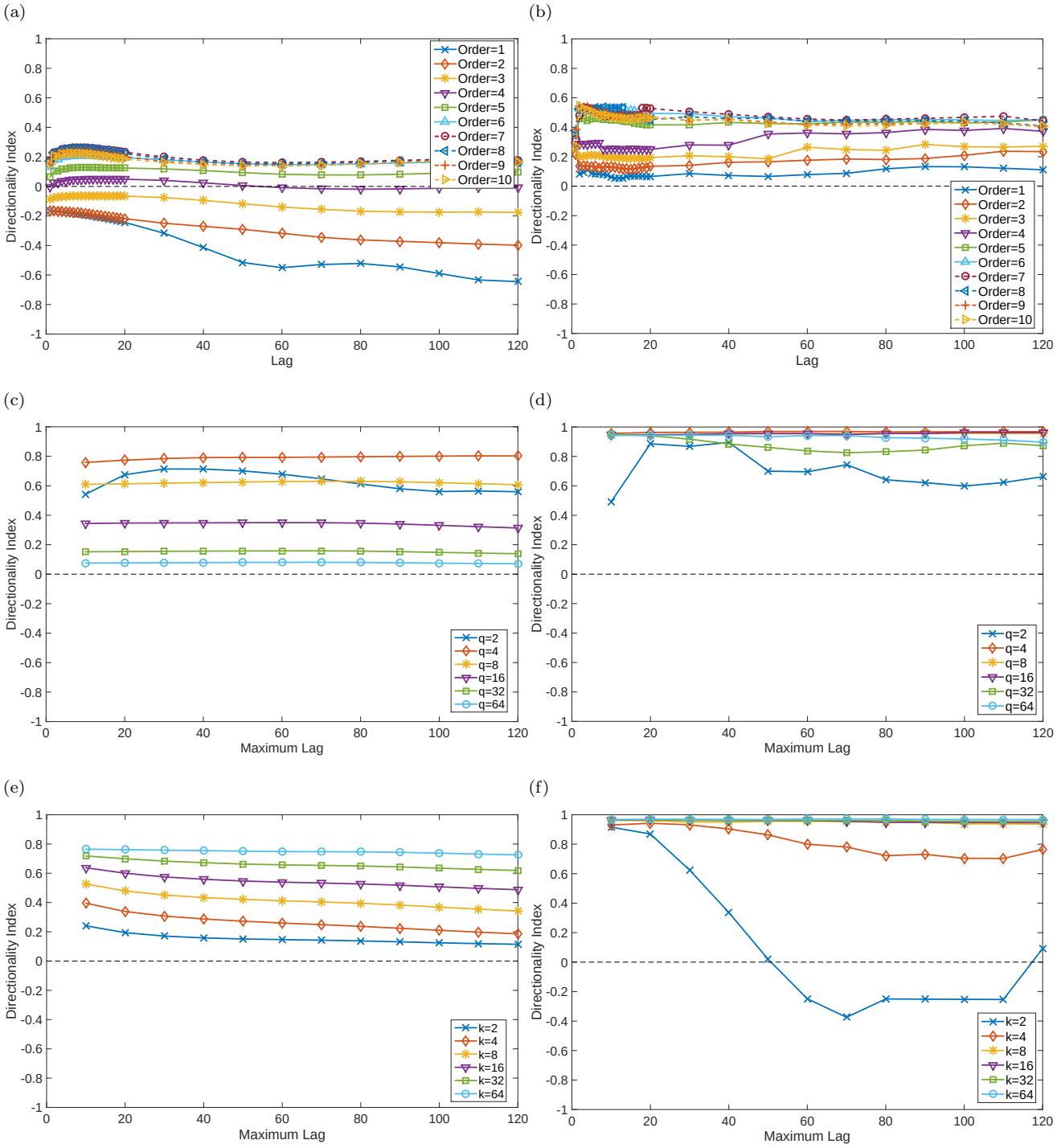

FIG. 2. Directionality indices averaged over 100 initializations for System 1: Rössler oscillators with unidirectional coupling from oscillator 1 to oscillator 2 (positive directionality indices) using a range of parameters of the different estimation methods. The left hand plots display the original directionality indices while the right hand plots are the recalibrated directionality indices. Top row: EMA; Middle row: CMI; bottom row: CMI-kNN.

shows the results of the directionality tests for coupling between oscillators of different frequencies as described in Section IV A, Systems 2 and 3. In this case for the CMI algorithm, with $q = 4$, when the coupling was from the fast to slow oscillator (direction $2 \rightarrow 1$) there were at least 40% of the results in the direction $1 \rightarrow 2$ which were outside of the range of the surrogates. However, this has no impact on the recalibrated directionality in-

TABLE II. Comparison of most successful parameters of the algorithms for a range of different lags/maximum lag for System 1: Rössler systems with unidirectional coupling from oscillator 1 to oscillator 2.

Algorithm	Parameters	% Correct		% Outside Surrogates		
		Original	Recalibrated	Original $D_{1\to2}$	$1 \to 2$	$2 \to 1$
EMA	order = 9	[73, 93]	[8, 33]	[9, 33]	[9, 33]	[9, 33]
CMI	$q = 16$	100	100	[85, 100]	100	[5, 7]
CMI-kNN	$k = 32$	100	100	[82, 99]	100	[7, 8]

TABLE III. Example results for Systems 2 and 3 with coupling between oscillators of different frequencies for EMA with order = 3, CMI with $q = 4$ and CMI-kNN with $k = 16$ across a range of lags/maximum lag. System 2 with coupling from the slower to faster oscillator (oscillator 1 to oscillator 2) results in a positive directionality index, System 3 with coupling from the faster to slower in a negative directionality index.

	Avg $D_{1\to2}$		% Correct		% Outside Surrogates		
	Original	Recalibrated	Original	Recalibrated	Orig $D_{1\to2}$	$1 \to 2$	$2 \to 1$
EMA							
slow to fast	[0.06, 0.41]	[−0.65, −0.08]	[66, 91]	[0, 5]	[10, 22]	[10, 22]	[10, 22]
fast to slow	[−0.18, 0.70]	[−0.63, 0.00]	[0, 83]	[0, 1]	[0, 5]	[0, 5]	[0, 5]
CMI							
slow to fast	[0.88, 0.94]	[1.00, 1.00]	100	100	100	100	[1, 3]
fast to slow	[−0.99, −0.98]	[−0.99, −0.99]	100	100	0	[43, 49]	100
CMI-kNN							
slow to fast	[0.94, 0.97]	[0.99, 1.00]	100	100	0	100	[1, 2]
fast to slow	[−1.00, −1.00]	[−1.00, −1.00]	100	100	[0, 1]	[15, 21]	100

dices with 100% in the correct direction with a value on average of -0.99. Comparing this with the results of the original directionality index where although the directionality indices were again all in the correct direction with similar average values, the results indicated that non of these values were outside of the range of the surrogate data.

The values of the order of the EMA algorithm and the parameters q and k of the CMI algorithms given in Table III were chosen as they provided the largest number of results, in the opposite direction to coupling, that were outside of the range of the surrogates and particularly highlight the differences between the proposed recalibrated estimator and the original estimator. Figure 3 shows the ranges of the surrogate data and average values of the coupling along with the corresponding original directionality indices and their surrogates for a range of different lag values for the EMA algorithm with order=3. The EMA algorithm displayed a wide range of variability both in the original and the recalibrated versions with a higher percentage of correctly identified directions of coupling from the original directionality index, however, the percentage of results outside of the range of the surrogates was the same for both versions and lower than for either of the CMI algorithms.

Figure 4 and Fig. 5 show the same information for the CMI with $q =$ and CMI-kNN with $k = 16$ respectively. Unlike the CMI estimator the CMI-kNN estimator has lower percentages of results outside of the range of the surrogates, for the opposite direction to the coupling. In these scenarios there were a maximum of 21% of the results in the direction opposite to the coupling that were outside the range of the surrogates but again 100% of directionality indices were in the correct direction with average values close to 1 or -1. As with the CMI algorithm the original CMI-kNN directionality indices gave similar results to the recalibrated but with a maximum of 1% of the results being outside of the range of the coupling.

B. Bidirectional Coupling

As a final test of the effectiveness of the new corrected directionality indices we analyzed three systems with bidirectional coupling as described in Systems 4-6 in Section IV A. As the directionality indices produce continuous values from −1 to 1, to distinguish between directionality in each direction and equivalent coupling, which should give a value of close to zero, thresholds were set at −0.25 and 0.25. Table IV shows the percentage of the test data sets across the range of maximum lag values tested, which are determined to have coupling in each direction (values either over 0.25 or below −0.25) or equivalent coupling (between −0.25 and 0.25). For the proposed directionality indices only we also show the

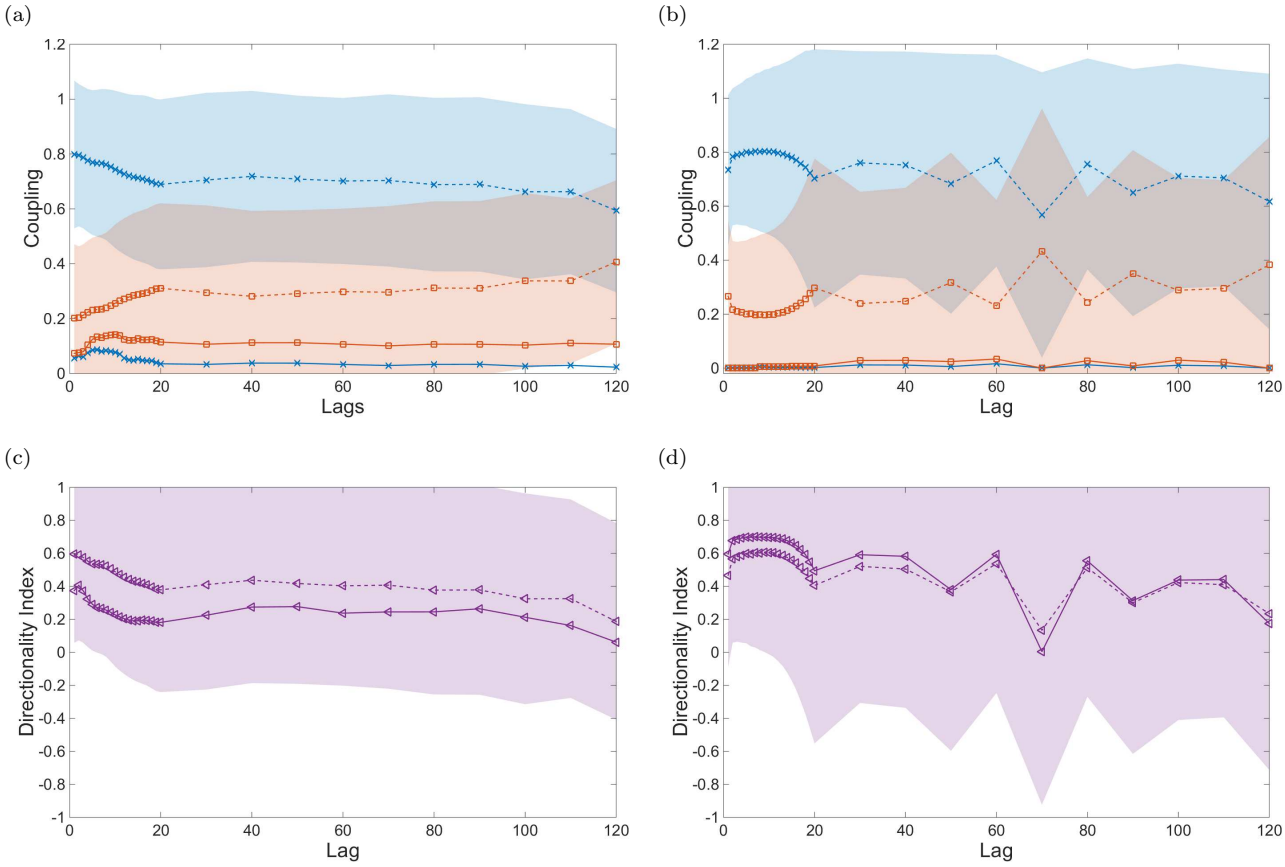

FIG. 3. Information transfer using EMA, order= 3 for coupled Rössler systems with a frequency ratio of 1:5. Plots on the left are coupling from fast to slow (positive directionality index) and on the right from slow to fast (negative directionality index). Top row shows the average recalibrated coupling in each direction. Blue (crosses) solid line: average recalibrated coupling in the direction $1 \rightarrow 2$, dashed line: average coupling from surrogates in the direction from $1 \rightarrow 2$, shaded area: 95% range of the surrogate data. Red (squares) lines in the direction $2 \rightarrow 1$. Bottom row shows the average original directionality indices. Solid line: average original directionality index, dashed line: average directionality index from the surrogates, shaded area: 95% range of the surrogate data.

percentage which are identified as having no coupling, the original directionality indices assume that the systems are coupled and only provides an indication of the direction of that coupling.

As with the unidirectional coupling the EMA algorithm had a wide range of results with no consistently correct indication of the direction of coupling. For all three systems and both formulations the maximum percentage of results outside of the range of the surrogate data was 68%. The original formulation of the directionality index was most likely to say the bidirectional coupling was equivalent coupling (based on our selected thresholds). With the recalibrated directionality index more likely to give a result of no coupling.

For Systems 4 and 5 the coupling in both cases was bidirectional but with different strengths and with the predominant direction of coupling in opposite directions from $1 \rightarrow 2$ for System 4 and from $2 \rightarrow 1$ for System 5. From Table IV we can see the recalibrated directionality indices calculated using the CMI algorithm successfully identified the directions of weak bidirectional coupling. There were only a small number of results below the thresholds to be considered equivalent coupling. In the same scenarios the original directionality index identified the coupling as equivalent coupling in all cases. For all situations and both formulations of the directionality indices 100% of the results were outside of the range of the surrogate data.

If we compare the results of the CMI-kNN algorithm in Table IV, again the original formulation of the directionality index was most likely to indicate that the coupling was equivalent. Although this time with a lower percentage of results outside of the range of the surrogates. This pattern was continued for the recalibrated directionality index where, in the situations where the results were outside of the range of the surrogate data, the direction would most likely be correct. However, again there was a higher probability when using this algorithm that neither of the measures of information transfer would be outside of the range of the surrogate data. Hence, the directio-

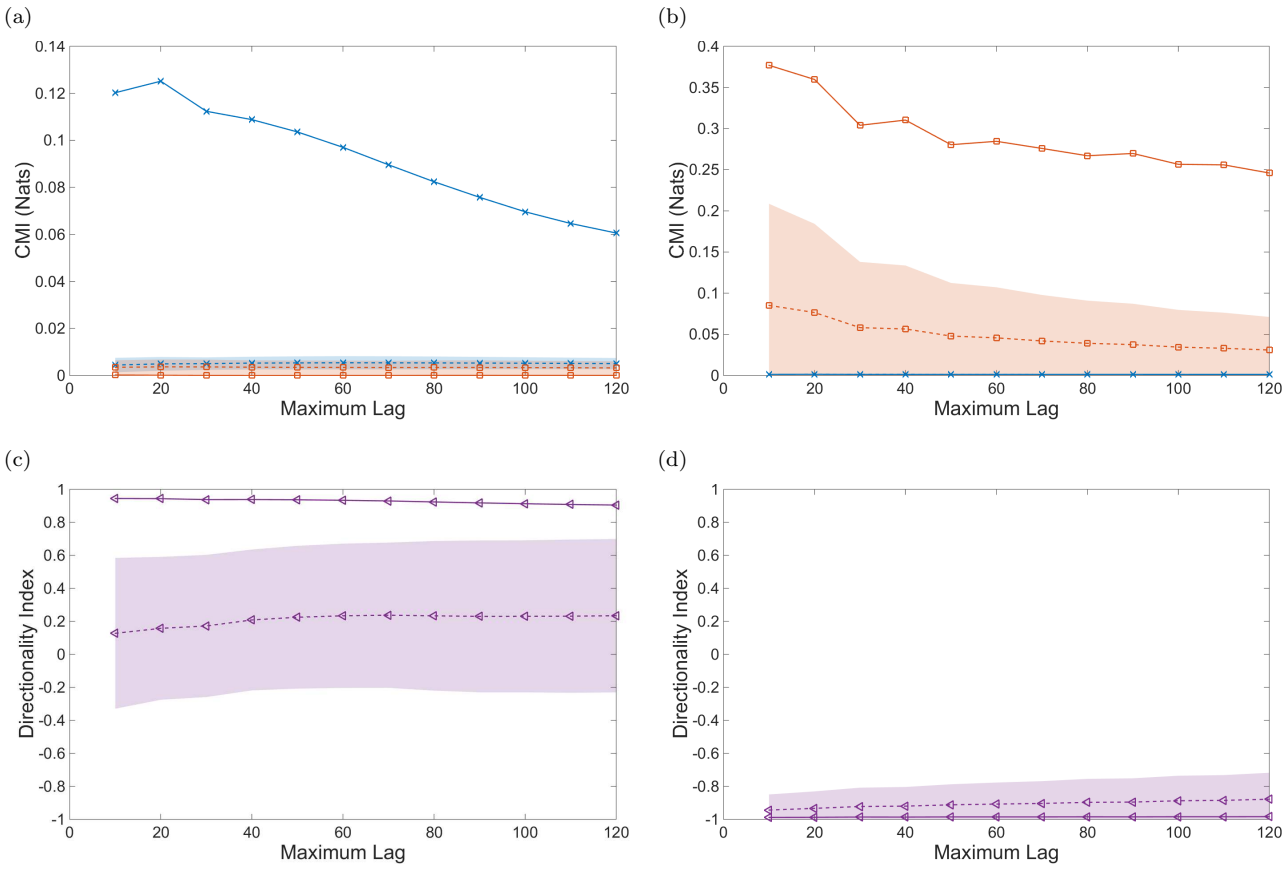

FIG. 4. Information transfer using CMI, $q = 4$ for coupled Rössler systems with a frequency ratio of 1:5. Plots on the left are coupling from fast to slow (positive directionality index) and on the right from slow to fast (negative directionality index). Top row shows the average recalibrated coupling in each direction. Blue (crosses) solid line: average recalibrated information in the direction $1 \rightarrow 2$, dashed line: average information from surrogates in the direction from $1 \rightarrow 2$ shaded area: 95% range of the surrogate data. Red (squares) lines in the direction $2 \rightarrow 1$. Bottom row shows the average original directionality indices. Solid line: average original directionality index, dashed line: average directionality index from the surrogates, shaded area: 95% range of the surrogate data.

nality index would indicate that there was no coupling. These results illustrate that even for a correctly calculated directionality index the choice of algorithm used to create the estimator remains still important.

The final system, System 6, with equivalent coupling, was correctly identified using the original formulation of the directionality index 100% of the time for the CMI algorithm and at least 99% of the time for the CMI-kNN. It should be noted, however, this formulation identified all bidirectional coupling as equivalent. Comparing the two algorithms again the CMI-kNN had a lower percentage of the results which were outside of the range of the surrogate data and could be considered significant. Using either algorithm the recalibrated index did not manage to reliably identify the equivalent coupling with both estimators more often identifying the equivalent coupling as a larger coupling in the direction $1 \rightarrow 2$. This, may of course be related to a bias in the estimators rather than a direct limitation in the calculation of the directionality indices.

VI. CONCLUSION

We have studied the use of directionality indices as a method of demonstrating the asymmetry in coupling between systems. Our results indicate that it is necessary to consider using appropriate tests of the significance of any results before inferring directionality of coupling. We propose a corrected directionality index which uses surrogate data testing to ensure valid results. This is achieved by factoring in differences between the results obtained when using the surrogate data to test the individual measures of coupling versus testing the directionality index directly. We have compared our proposed recalibrated directionality index with results from the original directionality index to show that the our proposed correction gives results which are more consistently significant for the tested systems and methods.

We compared two different methods of estimating coupling in order to generate the directionality indices: the modeling based EMA and a CMI approach to calculating

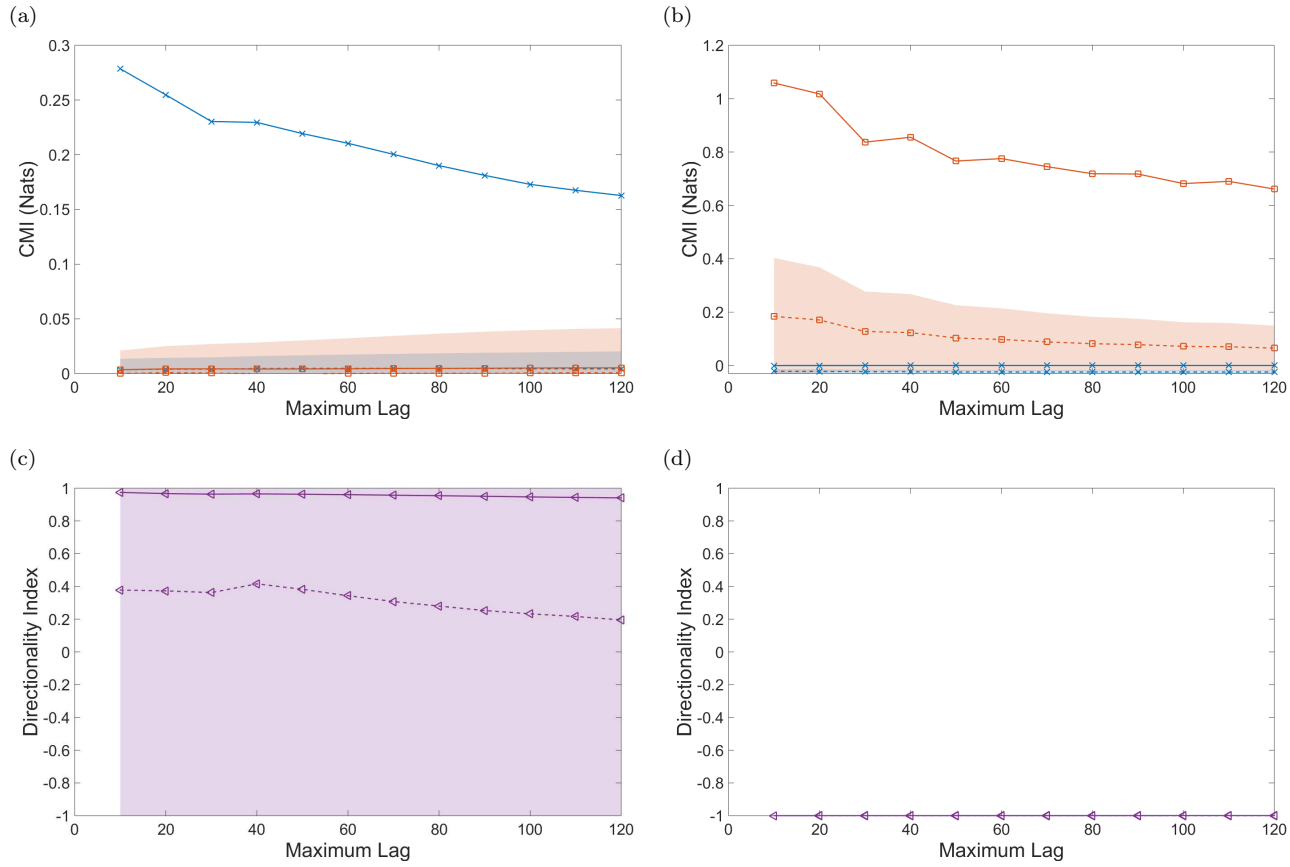

FIG. 5. Information transfer using CMI-kNN, $k = 16$ for coupled Rössler systems with a frequency ratio of 1:5. Plots on the left are coupling from fast to slow (positive directionality index) and on the right from slow to fast (negative directionality index). Top row shows the average recalibrated coupling in each direction. Blue (crosses) solid line: average recalibrated information in the direction $1 \to 2$, dashed line: average information from surrogates in the direction from $1 \to 2$ shaded area: 95% range of the surrogate data. Red (squares) lines in the direction $2 \to 1$. Bottom row shows the average original directionality indices. Solid line: average original directionality index, dashed line: average directionality index from the surrogates, shaded area: 95% range of the surrogate data.

TABLE IV. Example results of coupling between oscillators with bidirectional coupling, Systems 4-6, for EMA order = 3, CMI $q = 64$ and CMI-kNN $k = 8$. For each of the three scenarios: weak coupling stronger from $1 \to 2$, very weak coupling stronger from $2 \to 1$ and equivalent coupling the table provides the percentages identified as in the direction 1 to 2, direction 2 to 1, equivalent coupling or no coupling along with the percentages outside of the range of the surrogate data.

	% $1 \to 2$		% $2 \to 1$		% Equivalent		% No Coupling		% Outside Surrogates		
	Orig	Recal	Orig	Recal	Orig	Recal	Orig	Recal	Orig $D_{1\to2}$	$1 \to 2$	$2 \to 1$
EMA											
weak $1 \to 2$	[11, 35]	[11, 35]	[3, 14]	[0, 1]	[56, 77]	[0, 28]	N/A	[44, 88]	[12, 56]	[12, 56]	[12, 56]
very weak $2 \to 1$	[23, 45]	0	[0, 16]	[0, 16]	[42, 74]	[30, 60]	N/A	[33, 68]	[32, 67]	[32, 67]	[32, 67]
equivalent	[25, 41]	[13, 41]	[1, 10]	0	[49, 71]	[0, 34]	N/A	[37, 87]	[13, 68]	[13, 68]	[13, 68]
CMI											
weak $1 \to 2$	0	[89, 92]	0	0	100	[8, 11]	N/A	0	100	100	[8, 11]
very weak $2 \to 1$	0	0	0	[82, 85]	100	[15, 18]	N/A	0	100	[15, 18]	100
equivalent	0	[83, 90]	0	0	100	[10, 17]	N/A	0	100	100	[10, 17]
CMI-kNN											
weak $1 \to 2$	[0, 9]	[8, 63]	0	[5, 10]	[91, 100]	[1, 4]	N/A	[26, 80]	[6, 37]	[12, 65]	[9, 14]
very weak $2 \to 1$	[0, 1]	[0, 8]	0	[64, 80]	[99, 100]	[12, 34]	N/A	[0, 16]	[56, 100]	[19, 36]	[77, 100]
equivalent	[0, 10]	[37, 90]	0	[1, 5]	[99, 100]	[4, 13]	N/A	[2, 56]	[14, 77]	[42, 96]	[7, 14]

dynamic information rates. These methods were selected as both have previously been used to calculate directionality indices. For the CMI based approach we also compared two different methods for estimating the CMI. Our results show that although the EMA has previously been used in conjunction with directionality indices, using surrogate data testing and our corrected directionality index the results of this approach are not consistently statistically valid. When comparing the two CMI based estimators it was found that for unidirectional coupling there was little difference between the two approaches. However, when analyzing bidirectional coupling the differences in the CMI estimators became more apparent with the quantization based approach proving more effective until the coupling became very weak. For very weak bidirectional coupling the kNN based approach proved more sensitive to detecting this coupling than the quantization based approach. In terms of equivalent bidirectional coupling both methods failed to correctly identify this coupling indicating a possible bias in the estimators. It should be noted that these are only two possible methods for calculating information transfer and the proposed corrected directionality index could be applied to any unidirectional estimator of information transfer.

We have also extended the k-nearest neighbors method described in [18] based on the approach in [41] to give a more precise estimator for higher dimensions. In the example systems used here, in order to provide a direct comparison between the EMA and the quantization estimator, the systems were only one dimensional. In this case the estimator reduced to the rectangular estimator from [18] adapted for CMI. Having addressed the use of the directionality index as a method for describing the relationship between systems it would be of interest to test the proposed extension of the CMI approach on multidimensional neural data.

Appendix: Extension of kNN estimator for CMI

Following a similar approach to the extension of the mutual information estimator for application to transfer entropy [41] we first consider the calculation of the Shannon entropy based on the Kozachenko-Leonenko estimator [18]. If we have N realizations x_i of random variable X with density function $\mu(x)$ the Shannon entropy can be given as

$$H(X) = -\int dx \mu(x) \log \mu(x), \tag{A.1}$$

which for an unbiased estimator $\widehat{\log \mu(x)}$ becomes

$$\hat{H}(X) = -\frac{1}{N}\sum_{i=1}^{N} \widehat{\log \mu(x_i)}. \tag{A.2}$$

If $\varepsilon(i)/2$ is the distance between any point x_i and its k^{th} nearest neighbor, then p_i and v_i are the mass and volume, respectively, of the hyper-ball with radius $\varepsilon(i)/2$ centered on the point x_i. Assuming the density $\mu(x)$ is constant within the entire ball then

$$p_i(\epsilon) \approx c_d \varepsilon^d \mu(x_i), \tag{A.3}$$

where d is the dimension of x and c_d is the volume of the d-dimensional unit ball. It can also be shown that the expectation value of $\log p_i(\varepsilon)$ can be given as [18]

$$E[\log p_i] = \psi(k) - \psi(N), \tag{A.4}$$

where ψ is the digamma function. Combining (A.3) and (A.4) gives

$$\begin{aligned} \psi(k) - \psi(N) \simeq & E\left[\log\left(c_d \varepsilon^d \mu(x_i)\right)\right] \\ = & E\left[\log \mu(x_i)\right] + E\left[\log\left(c_d \varepsilon^d\right)\right] \\ = & -H(X) + E\left[\log v_i\right], \end{aligned} \tag{A.5}$$

hence, giving

$$\hat{H}(X) = \psi(N) - \psi(k) + \frac{1}{N}\sum_{i=1}^{N} \log v_i. \tag{A.6}$$

The CMI calculated by the sum of entropies as defined in (12) requires estimates of the entropy in both the joint and marginal spaces. However, using the same value of k across all spaces can result in problems occurring because the biases in the estimates do not cancel due to calculating over different scales. In [18] it was noted that the entropy estimator (A.6) would hold for any value of k. Therefore, rather than calculating the entropies in both the joint and marginal spaces based on the same k, they could be calculated based on the same distance ε. The number of points, $n_x[i]$, within this region is defined as the points within the lines $x = x_i \pm \varepsilon(i)/2$ and the corresponding estimator becomes

$$\hat{H}(X) = \psi(N) + \frac{1}{N}\sum_{i=1}^{N} \Big(\log v_i - \psi\big(n_x[i]\big)\Big). \tag{A.7}$$

However, defining the spaces in this way results in a hyper-cube where the length of the sides, ε, are defined as twice the distance to the k^{th} nearest neighbor in the joint space, which means the estimates in the marginal spaces are only truly accurate for one variable. To overcome this the authors in [18] propose a second mutual information estimator using hyper-rectangles to define separate ε for each variable. For m variables, if $q_i(\varepsilon_{x_1}, ...\varepsilon_{x_m})$ is the mass of the hyper-rectangle of size $\varepsilon_{x_1} \times \varepsilon_{x_2} \times, \ldots, \varepsilon_{x_m}$ centered at $(x_{1,i}, x_{2,i}, \ldots, x_{m,i})$, then $E\left[\log q_i\right] = \psi(k) - (m-1)/k - \psi(N)$. In [41] the authors extended this principle from the estimation of mutual information of multivariate data to the estimation of entropy of multidimensional data. For data of dimension d the expectation of $\log q_i(\varepsilon_1, ..., \varepsilon_d)$ becomes

$$E\left[\log q_i\right] = \psi(k) - (d-1)/k - \psi(N), \tag{A.8}$$

and the entropy estimator

$$\hat{H}(X) = \psi(N) - \psi(k) + \frac{d-1}{k} - \frac{1}{N}\sum_{i=1}^{N} \log v_i, \quad \text{(A.9)}$$

where v_i is now the volume of the minimum volume hyper-rectangle centred at x_i.

If we consider the CMI of three multidimensional random variables X, Y and Z, then, based on (A.9) the entropy estimator in the joint space is given by

$$\hat{H}(X,Y,Z) = \psi(N) - \psi(k) + \frac{d_x + d_y + d_z - 1}{k} + \frac{1}{N}\sum_{i=1}^{N} \log v_i. \quad \text{(A.10)}$$

In the marginal spaces (X,Z), (Y,Z) and Z using the same dimensions of the minimal hyper-rectangle as for the joint space and estimators based on an arbitrary number of points as in (A.7) then we have

$$\hat{H}(X,Z) = \psi(N) + \frac{1}{N}\sum_{i=1}^{N} \Big(\log v_i - \psi\big(n_{xz}[i]\big) + \frac{d_x + d_z - 1}{n_{xz}[i]} \Big), \quad \text{(A.11)}$$

$$\hat{H}(Y,Z) = \psi(N) + \frac{1}{N}\sum_{i=1}^{N} \Big(\log v_i - \psi\big(n_{yz}[i]\big) + \frac{d_y + d_z - 1}{n_{yz}[i]} \Big), \quad \text{(A.12)}$$

$$\hat{H}(Z) = \psi(N) + \frac{1}{N}\sum_{i=1}^{N} \Big(\log v_i - \psi\big(n_z[i]\big) + \frac{d_z - 1}{n_z[i]} \Big), \quad \text{(A.13)}$$

resulting in the estimator of the CMI as given in (13).

ACKNOWLEDGMENTS

This work was fully supported by the Research Grants Council of the Hong Kong Special Administrative Region, China [Project No. CityU110813] and a grant from the Croucher Foundation.

[1] A. Zaremba and T. Aste, Entropy **16**, 2309 (2014).
[2] G. Sugihara, R. May, H. Ye, C.-h. Hsieh, E. Deyle, M. Fogarty, and S. Munch, Science **338**, 496 (2012).
[3] R. Quian Quiroga, A. Kraskov, T. Kreuz, and P. Grassberger, Phys. Rev. E **65**, 041903 (2002).
[4] J. Dauwels, F. Vialatte, T. Musha, and A. Cichocki, NeuroImage **49**, 668 (2010).
[5] M. Paluš, V. Komárek, T. Procházka, Z. Hrnćir, and K. Šterbová, IEEE Eng. Med. Biol. Mag. **20**, 65 (2001).
[6] D. Dentico, B. L. Cheung, J.-Y. Chang, J. Guokas, M. Boly, G. Tononi, and B. Van Veen, NeuroImage **100**, 237 (2014).
[7] J. R. Sato, D. Y. Takahashi, S. M. Arcuri, K. Sameshima, P. A. Morettin, and L. A. Baccalá, Hum. Brain Mapp. **30**, 452 (2009).
[8] H. Zhang, H. L. Benz, N. V. Thakor, and A. Bezerianos, Int. J. Bifurct. Chaos **22**, 1250225 (2012).
[9] A. Korzeniewska, C. M. Crainiceanu, R. Kuś, P. J. Franaszczuk, and N. E. Crone, Hum. Brain Mapp. **29**, 1170 (2008).
[10] N. V. Manyakov and M. M. V. Hulle, in *Proc. ESANN 2007, 15th European Symposium on Artificial Neural Networks* (d-side publi., Bruges (Belgium), 2007) pp. 447–452.
[11] A. Korzeniewska, S. Kasicki, M. Kamiński, and K. Blinowska, J. Neurosci. Methods **73**, 49 (1997).
[12] A. Korzeniewska, M. Mańczak, M. Kamiński, K. J. Blinowska, and S. Kasicki, J. Neurosci. Methods **125**, 195 (2003).
[13] K. J. Blinowska, Med. Biol. Eng. Comput. **49**, 521 (2011).
[14] C. W. J. Granger, Econometrica **37**, 424 (1969).
[15] P. J. Franaszczuk, K. J. Blinowska, and M. Kowalczyk, Biol. Cybern. **51**, 239 (1985).
[16] M. J. Kaminski and K. J. Blinowska, Biol. Cybern. **65**, 203 (1991).
[17] J.-P. Lachaux, E. Rodriguez, J. Martinerie, and F. J. Varela, Hum. Brain Mapp. **8**, 194 (1999).
[18] A. Kraskov, H. Stögbauer, and P. Grassberger, Phys. Rev. E **69**, 066138 (2004).
[19] A.-K. Seghouane and S.-I. Amari, IEEE Trans. Neural Netw. **18**, 97 (2007).
[20] T. Schreiber, Phys. Rev. Lett. **85**, 461 (2000).
[21] T. Kreuz, F. Mormann, R. G. Andrzejak, A. Kraskov, K. Lehnertz, and P. Grassberger, Physica D **225**, 29 (2007).
[22] G. B. Ermentrout and C. C. Chow, Physiol. Behav. **77**, 629 (2002).
[23] M. Lobier, F. Siebenhühner, S. Palva, and J. M. Palva, NeuroImage **85**, 853 (2014).
[24] M. G. Rosenblum and A. S. Pikovsky, Phys. Rev. E **64**, 045202 (2001).
[25] M. Paluš and A. Stefanovska, Phys. Rev. E **67**, 055201 (2003).
[26] J. T. Lizier and M. Prokopenko, Eur. Phys. J. B **73**, 605 (2010).
[27] D. Chicharro and A. Ledberg, PLoS ONE **7**, e32466 (2012).
[28] M. Wibral, R. Vicente, and M. Lindner, in *Directed*

Information Measures in Neuroscience, Understanding Complex Systems, edited by M. Wibral, R. Vicente, and J. T. Lizier (Springer Berlin Heidelberg, 2014) pp. 3–36.
[29] P. Wollstadt, M. Martínez-Zarzuela, R. Vicente, F. J. Díaz-Pernas, and M. Wibral, PLoS ONE **9**, e102833 (2014).
[30] M. Zhang, C. Zheng, M. Quan, L. An, Z. Yang, and T. Zhang, Neurosignals **19**, 189 (2011).
[31] C. Zheng and T. Zhang, Neuroscience **292**, 170 (2015); C. Zheng, M. Quan, and T. Zhang, J. Comput. Neurosci. **33**, 547 (2012).
[32] B. Musizza, A. Stefanovska, P. V. E. McClintock, M. Paluš, J. Petrovčič, S. Ribarič, and F. F. Bajrović, J. Physiol. **580**, 315 (2007).
[33] L. Cimponeriu, M. G. Rosenblum, T. Fieseler, J. Dammers, M. Schiek, M. Majtanik, P. Morosan, A. Bezerianos, and P. A. Tass, Prog. Theor. Phys. Supp. **150**, 22 (2003).
[34] M. G. Rosenblum, L. Cimponeriu, A. Bezerianos, A. Patzak, and R. Mrowka, Phys. Rev. E **65**, 041909 (2002).
[35] D. A. Smirnov and B. P. Bezruchko, Phys. Rev. E **68**, 046209 (2003).
[36] D. A. Smirnov and R. G. Andrzejak, Phys. Rev. E **71**, 036207 (2005).
[37] M. Paluš, V. Komárek, Z. Hrnčíř, and K. Štěrbová, Phys. Rev. E **63**, 046211 (2001).
[38] K. Hlaváčková-Schindler, M. Paluš, M. Vejmelka, and J. Bhattacharya, Phys. Rep. **441**, 1 (2007).
[39] M. Vejmelka and M. Paluš, Phys. Rev. E **77**, 026214 (2008).
[40] I. Vlachos and D. Kugiumtzis, Phys. Rev. E **82**, 016207 (2010).
[41] J. Zhu, J.-J. Bellanger, H. Shu, and R. Le Bouquin Jeannès, Entropy **17**, 4173 (2015).
[42] O. Rössler, Phys. Lett. A **57**, 397 (1976).
[43] M. G. Rosenblum, A. S. Pikovsky, and J. Kurths, Phys. Rev. Lett. **76**, 1804 (1996).
[44] M. Paluš, Phys. Lett. A **235**, 341 (1997).
[45] J. Theiler, S. Eubank, A. Longtin, B. Galdrikian, and J. D. Farmer, Physica D **58**, 77 (1992).
[46] T. Schreiber and A. Schmitz, Physica D **142**, 346 (2000).
[47] T. Schreiber and A. Schmitz, Phys. Rev. Lett. **77**, 635 (1996).
[48] M. Paluš and M. Vejmelka, Phys. Rev. E **75**, 056211 (2007).